

# Physical Properties and Structure of Unreacted PC/PBT Blends

P. SÁNCHEZ, P. M. REMIRO, and J. NAZÁBAL\*

Departamento de Ciencia y Tecnología de Polímeros, Facultad de Química. (EHU/UPV),  
P. O. Box 1072 20080-San Sebastian, Spain

## SYNOPSIS

Unreacted PC/PBT blends have been obtained by melt blending in all the composition ranges. The followed processing method produced partially miscibilized and crystalline blends. The plot of the density of the amorphous part of the blends against its composition indicates that this parameter is more important than the crystallinity level in determining the mechanical properties of the blends. The blends exhibited an overall improvement of mechanical properties with a combination of behaviors that are close to linearity and are synergistic. © 1993 John Wiley & Sons, Inc.

## INTRODUCTION

There are many reasons why polymer blending is one of the most important areas in polymer research and development.<sup>1,2</sup> Among these reasons, the most important is, perhaps, that polymer blends offer a fast and cheap way to obtain new polymeric materials. These materials generally exhibit a range of properties that varies between those of the components. Moreover, their properties may be complementary and difficult to find together in the case of a single component.

Blends of condensation polymers, like polyesters or related materials, have given rise to considerable research work in the last few years.<sup>3,4</sup> This is because these blends, besides having the usual characteristics of polymer blends, are able to react under processing conditions<sup>5</sup> to produce copolymers. These copolymers are products that can clearly improve the mechanical compatibility of the blends because they contain both components of the blends. For these reasons, much work has been done with the aim of understanding the way and conditions for these reactions to be produced.

Among the blends of polyesters and related materials, the blends between polycarbonate (PC) and

poly(butylene terephthalate) (PBT) have been, perhaps, the most widely studied since 1978.<sup>6,7</sup> This is because of the particular interest of the blend itself<sup>4-18</sup> as well as its studies in general works of interchange reactions.<sup>8</sup>

PC/PBT blends are partially miscible blends that can develop interchange reactions when they are melt-mixed. The produced reaction is a direct transesterification<sup>8</sup> that gives rise to the production of random and block PC/PBT copolymers. This reaction is dependent on the reaction time and temperature. The miscibility behavior and the interchange reactions that may be produced have been widely studied as well as the morphology<sup>7</sup> of the blends and the morphology and deformation behavior of the toughened blends.<sup>9</sup> Moreover, PC/PBT blends are commercialized under the trade names of Xenoy (General Electric) and Makroblend (Bayer). A work on the mechanical properties of Xenoy<sup>10</sup> has also been published; however, no work to our knowledge has been published dealing with the mechanical properties of unreacted or reacted blends as a function of composition.

This is why we have produced melt-mixed unreacted blends. The aim is to discover the mechanical properties of the blends in their unreacted raw state and in all the composition ranges. The crystalline content of the blends and the phase behavior itself have been discussed. The former has a great influence on the phase behavior, and the latter, on

\* To whom correspondence should be addressed.

the mechanical properties of the blends. The mechanical properties of the reacted blends will be the subject of a following work.

## EXPERIMENTAL

The used PC, Makrolon 2805 (Bayer), and PBT, Arnite T06-200 (Akzo Plastics), were dried at 120°C for a minimum of 48 h before melt blending. Blending was carried out in a Brabender Plasticorder PLE 650 at 30 rpm and 280°C. In Figure 1, the log torque–time curves of the pure components and that of the 50/50 blend are plotted. As can be seen, the torque obtained for the pure PC is fairly constant with time. This is to be expected because of the known stability of PC. However, the relative decrease of the torque, as a result of the viscosity of PBT, is a clear indication of degradation. A minimum blending time of 8 min has been chosen because this will allow effective blending and a minimum, if any, degradation to occur. After melt blending, the blends were compression-molded at 260°C using a Schwabenthan Polystat 200 T press. From the square sheets

obtained, specimens for measurement of properties were extracted.

Dynamic mechanical tests were performed in a DMTA (Polymer Laboratories) in single cantilever mode at 1 Hz and at a scan rate of 4°C/min. The storage modulus  $E'$ , the loss modulus  $E''$ , and the  $\tan \delta$  were obtained. DSC scans of the blends were performed in a calorimeter DuPont 990 at a scan rate of 20 K/min. The glass transition, melting, and crystallization temperatures as well as the crystallization and melting heats were obtained from the scans.

Tensile specimens (ASTM D638, type IV) were punched out by a pneumatic machine. Tensile tests were performed in an Instron 4301 at a speed of 10 mm/min and at room temperature. The Young's modulus  $E$ , yield stress  $\sigma_y$ , break stress  $\sigma_b$ , and ductility  $\epsilon_b$  (measured as elongation at break) were obtained from the nominal  $\sigma$ – $\epsilon$  plots. A minimum of 10 specimens was tested for each reported value.

The fracture surfaces of the tensile specimens were observed after gold coating in a scanning electron microscope (Hitachi S-2700) at 15 kV. The biphasic nature of the blends was not directly observ-

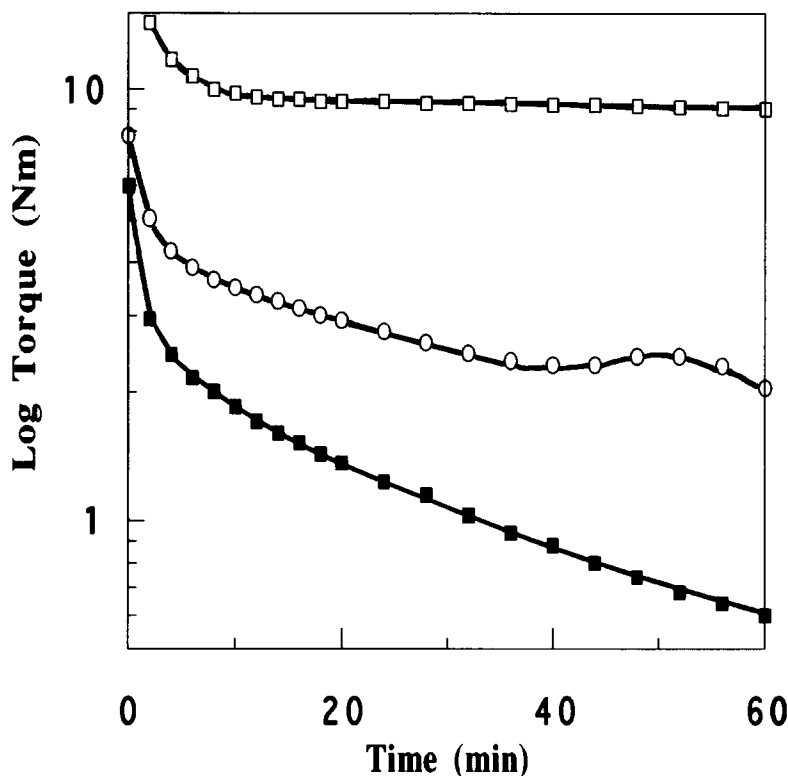


**Figure 1** Logarithmic torque of blending vs. time curves of PC (empty squares), PBT (solid squares), and a 50/50 blend (empty circles).

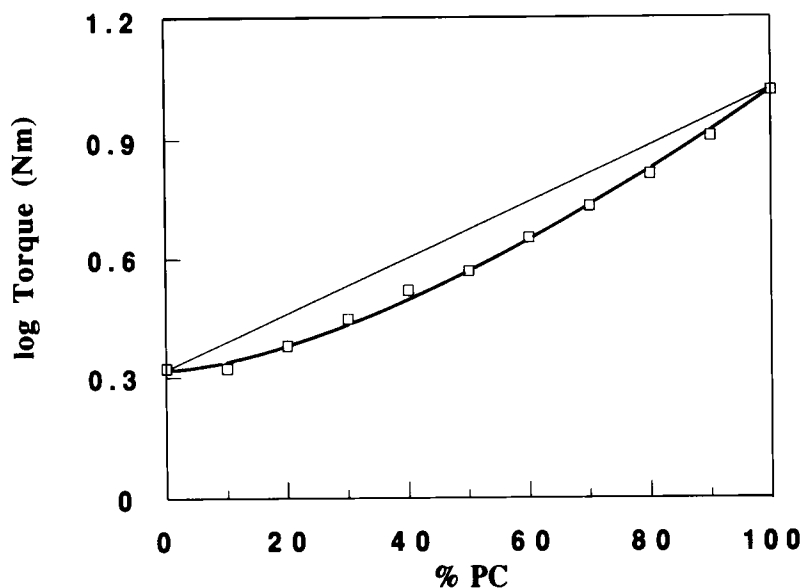


Figure 2 Plot of the logarithmic torque of blending vs. blend composition.

able, so the surfaces were etched with diethylene-triamine, which selectively attacks the PC phase.

## RESULTS AND DISCUSSION

### Nature of the Blends and Torque of Blending

The unreacted nature of the blends has been proven by solubility tests. In the case of the used PBT, and opposite to other PBTs, fairly long mixing times were necessary for any sign of reaction to be observed by the torque behavior. However, solubility tests are necessary because interchange reactions have been easily produced under these conditions<sup>8</sup> due mainly to the presence of catalyst residues. The tests were performed using methylene chloride, a good PC solvent that does not dissolve PBT. The obtained solubility values were very close to the PC content of the blends. It can be concluded that the melt-blending method produces essentially unreacted blends.

All the PC/PBT blends in the melted state at 280°C were transparent. This transparency was maintained in the solid state in PC-rich blends. Meanwhile, the PBT-rich blends, although translucent, were not fully transparent. Transparency is usually an indication of miscibility. However, it must be taken into account that the refraction indices of both components (1.586 for PC and 1.587 for PBT) are almost the same. This fact will probably be the only reason for the observed transparency of the blends.

In Figure 2, the torque, after a blending time of 8 min, is plotted against blend composition. As can be seen, the torque is always below linearity. Although exceptions are not rare,<sup>13</sup> this agrees with the attempts<sup>11,12</sup> that predict the following: positive deviations from the log-additivity rule in the case of miscible blends and negative deviations in the case of immiscibility or partial miscibility.

### Phase Behavior

The crystalline content of the blends and sometimes the phase behavior are dependent on the processing method followed.<sup>19</sup> Because of their influence on the mechanical properties, both the phase behavior and the crystalline content were studied using the dynamic-mechanical (DMTA) and calorimetric (DSC) results.

In Figure 3, the  $T_g$ 's of the blends obtained from the  $\tan \delta$  peaks by DMTA are shown against blend composition for both the first and second scans. During the first scan, distinct additional crystallizations were observed, indicating the lack of full crystallization in all the molded blends. If we look at the first scan  $T_g$  values, two  $T_g$ 's appear in the composition range. The different  $T_g$  values of the blends, related to those of the pure components, indicate the presence of both components in each phase of the blend. As is well known, this is a partially miscible blend. The  $T_g$  of the PBT-rich phase increases with pure PBT and then slowly decreases as the PC contents increase. The  $T_g$  increase from

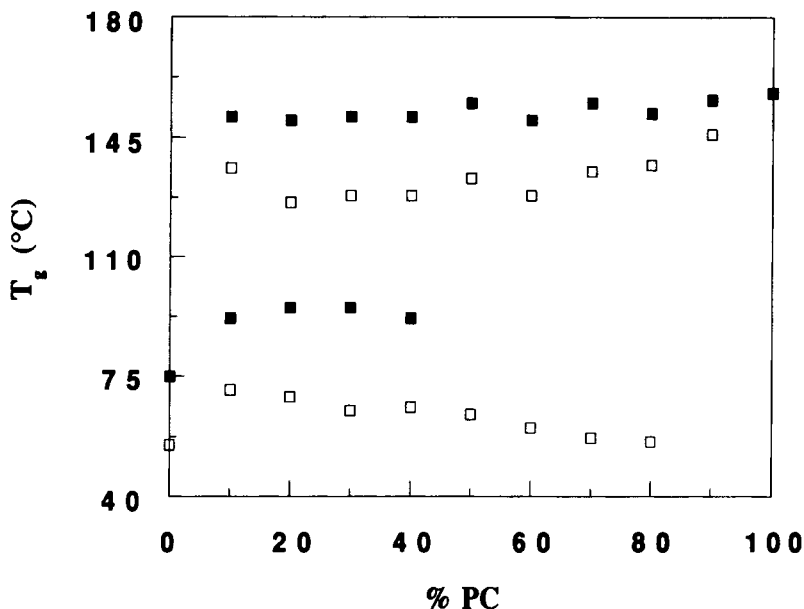


**Figure 3**  $T_g$ 's of the blends by DMTA: (empty squares) first scan; (solid squares) second scan.

that of pure PBT is a consequence of the presence of PC in the amorphous PBT phase. The following decrease will probably be a consequence of the decrease in the crystalline content of the PBT. This crystallinity decrease takes place at increasing PC contents of the overall blend and will be measured later. This decrease in the crystalline content leads to a decrease in the hindrance of the crystalline PBT to the movement of the amorphous PBT-rich phase.

It also leads to an increase in the amorphous PBT content of the blends. Both effects lead to a decrease in the  $T_g$  of the PBT-rich phases.

With respect to the  $T_g$  of the PC-rich phase, the usual decrease to a constant value is observed; thus, a constant maximum content of PBT in the phase is reached. The  $T_g$  of this composition constant PC-rich phase is roughly 130°C, as can be seen in Figure 3. The observed  $T_g$  values from the second scan are

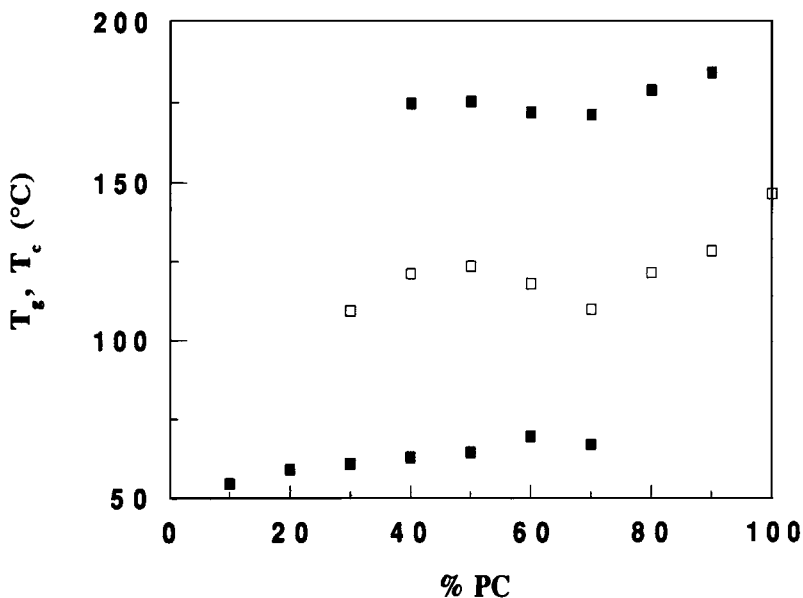


**Figure 4**  $T_g$ 's (empty squares) and  $T_c$ 's (solid squares) of the blends by DSC. The  $T_g$ 's of the PBT-rich phases are not shown.

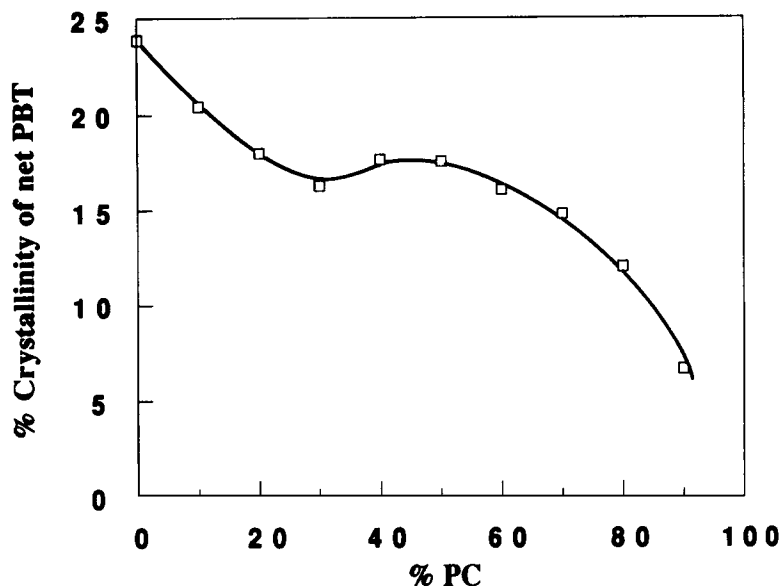


Figure 5 Percent crystallinity of net PBT vs. blend composition.

in accordance with the crystallization during the first scan. Observed were (a) a decrease in the PBT content of the PC-rich phase—thus, a  $T_g$  increase—and (b) an increase in the difficulty to move, as is seen in the  $T_g$  of the amorphous PBT. The latter is due to the increased amount of crystalline PBT. The  $T_g$  values of the amorphous PBT-rich phase of the PC-rich blends could not be measured due to the superimposed crystallization.

The  $T_c$  and  $T_g$  of the blends, as well as their crystalline content obtained by DSC, have been plotted, respectively, in Figures 4 and 5. The  $T_m$  values ob-

tained were relatively constant ( $222^\circ\text{C}$ ) and are not plotted. This consistency of the  $T_m$  indicates that the morphology of the crystalline PBT is basically the same regardless of its origin—PBT-rich phase, PC-rich phase, or melt blend—and its blend compositions.

In Figure 4, two different  $T_c$ 's can be seen. Each of them corresponds to crystallization from one of the two amorphous phases of the blend. This proves the lack of full crystallization of PBT during the molding process as well as the presence of PBT in the PC-rich phase. This presence of PBT in the PC-

Table I Crystalline PBT Content of the As-molded Blends and Crystallized PBT During Calorimetric Scan

Composition PC/PBT	As Molded		Calorimetric Scan		Total (%) <sup>b</sup>
	$X_{\text{PBTc}}$ <sup>a</sup>	(%) <sup>b</sup>	PBT-rich Phase (%) <sup>b</sup>	PC-rich Phase (%) <sup>b</sup>	
90/10	0.007	6.7		18.7	25.4
80/20	0.024	12.1		8.6	20.7
70/30	0.044	14.8	5.8	7.9	28.5
60/40	0.064	16.1	4.2	8.1	28.4
50/50	0.088	17.6	4.5	3.3	25.4
40/60	0.106	17.7	4.2	1.8	23.7
30/70	0.114	16.3	4.1		20.4
20/80	0.144	18.0	4.8		22.8
10/90	0.184	20.5	4.4		24.9
0/100	0.239	23.9			23.9

<sup>a</sup> Referred to the overall blend.

<sup>b</sup> Referred to the net PBT.

rich phase is large because, besides the observed  $T_g$  decrease, an important amount of PBT crystallizes from the PC-rich phase. As can be seen in Table I, this crystallized PBT amount is comparable to that crystallized from the PBT-rich phase. Table I shows the crystallinity of the as-molded blends, the amounts of crystallized PBT during the calorimetric scans from the two phases of the blends, and the total amount of crystalline PBT of the blends after the calorimetric scans.

With respect to the  $T_g$  behavior from DSC, the low-temperature  $T_g$  was affected by the enthalpic relaxation process and is not plotted. The  $T_g$  behavior of the PC-rich phases of the blends is different from that which was seen in Figure 3. This is because a small maximum, a trace of which was also seen in Figure 3, is seen at a roughly 50/50 composition. This is probably due to the maximum that is seen when the percent net crystallinity of PBT, which refers to only the PBT content of the blend,

against blend composition is plotted in Figure 5. As can be seen, the relative maximum in crystallinity observed in this plot also gives rise to a relative maximum hindrance to the movement of the amorphous phase. It also gives rise to a relative maximum in its  $T_g$  as is observed in Figure 4. Other small differences between the DSC and DMTA plots of the  $T_g$ 's are probably due to the different thermal profile during the scans.

### Morphology

The fracture surfaces of some representative tensile specimens are collected in Figure 6. Two distinct fracture zones were observed in the blend compositions: a ductile fracture zone and a brittle zone. The ductile fracture zone occurred close to the fracture nucleation site and, depending on composition, occupied roughly a third of the surface. The continuity of the brittle zone avoided the observation of

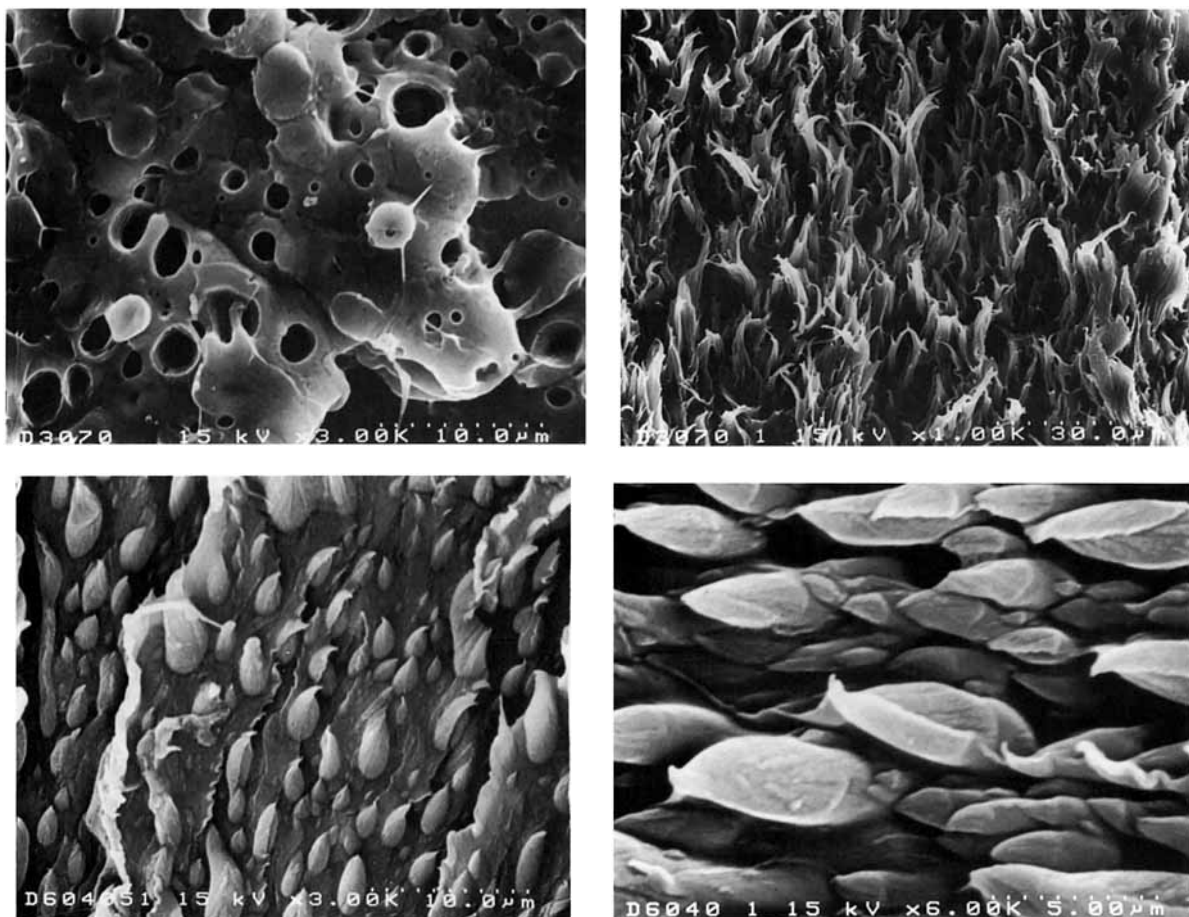


**Figure 6** Scanning electron micrographs of fracture surfaces of (a) etched brittle zone of a 30/70 blend, (b) etched ductile zone of a 30/70 blend and (c) nonetched, and (d) etched ductile zones of a 60/40 blend.

the dispersed phases that were revealed by etching. This appears in Figure 6(a), where the brittle zone of a 30/70 blend is shown. As can be seen, the holes reveal the presence of PC. The shape of the holes reveals a rodlike morphology that was also evident in the case of the PC-rich blends. This morphology is probably a consequence of the permanent deformation during the tensile test that was roughly 92%.

The morphology of Figure 6(b), corresponding to a 30/70 etched blend, reveals the ductile nature of the PBT matrix. More information is given by Figure 6(c) and (d), where 60/40 nonetched and etched specimens are shown. As can be seen, no holes or dewetting appear in the fracture surface and all the rods are clearly deformed and broken. This experimental evidence exhibits the exceptional adhesion level existent between the two phases. Produced is a breaking out of the dispersed phase in all cases and without any sign of dewetting. This process allows an effective incorporation of the properties of the dispersed phase to those of the blend.

### Mechanical Properties

With respect to the tensile curves, very sharp stress drops took place after yielding. This was the case of PBT and PBT-majority blends. Localized shear bands that gave rise to slower stress drops appeared in the case of PC and PC-majority blends. A mixed behavior took place in the case of the 50/50 blend. The width of the peak of yielding increased uniformly from that of pure PBT to that of pure PC.

The measured properties of the blends have been the modulus of elasticity, yield stress, break stress, and ductility, measured by deformation at break. The moduli of elasticity of the blends, as well as other mechanical properties, have often been related to density.<sup>20</sup> This is because densification, the loss of free volume, makes movement difficult at a segmental level. The result is an increase in stiffness, among other effects. However, in the case of crystalline polymers like PBT, the plot of density of the blends against composition is rather difficult to discuss. This is because the change of free volume concomitant with another parameter that influences density (i.e., the crystallinity level) changes with the composition of the blend. This is why in Figure 7 the density of the blends ( $\rho_b$ , empty squares) and that of only the amorphous part of the blends ( $\rho_a$ , solid squares) are shown. They are displayed as a function of composition together with the linear reference linking the density of PC with (a) that of the used PBT (1.289 g/cc) and (b) that of the amorphous PBT (1.258 g/cc).<sup>21</sup> The plot of the density of the amorphous part of the blends has been obtained from the following: the plot of the density of the overall blends, the crystalline content of the blends,  $X_{\text{PBTc}}$  from Table I, and the density of the fully crystalline PBT ( $\rho_{\text{PBTc}} = 1.396$  g/cc) using the expression

$$\frac{1}{\rho_b} = \frac{1 - X_{\text{PBTc}}}{\rho_a} + \frac{X_{\text{PBTc}}}{\rho_{\text{PBTc}}}$$

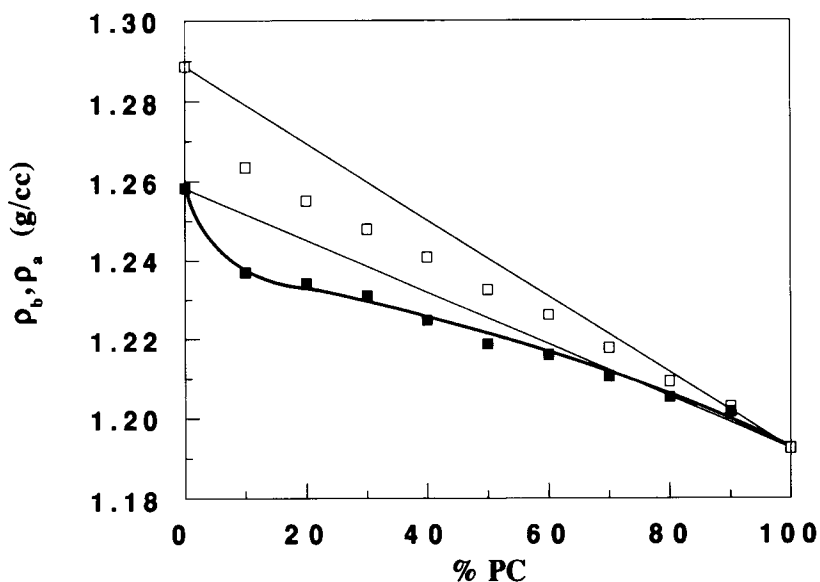


**Figure 7** Overall density of the blend  $\rho_b$  (empty squares) and density of the amorphous part of the blend  $\rho_a$  (solid squares) vs. blend composition.

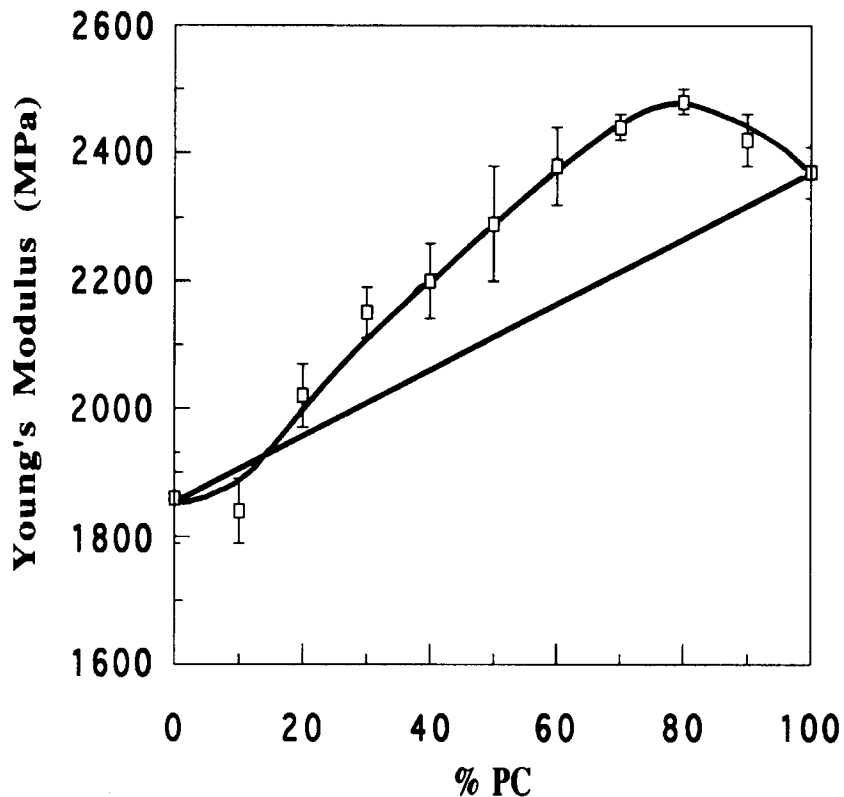


Figure 8 Tensile Young's modulus vs. blend composition.

Thus, the density of the amorphous part of the blends together with their crystalline content from Figure 5 and Table I will allow us to discuss the separate contribution of the change of free volume and of the crystalline level to the properties of the blends.

Referring to Figure 7, the density values of the blends ( $\rho_b$ , empty squares) appear under the plotted line connecting the density of the used PBT (1.289 g/cc) to that of the PC. With respect to the effect on  $\rho_b$  of the PBT crystalline level in the blends, its decrease will give rise to an increased separation of the density values of the blends from linearity. This decrease is relative to that of pure PBT (plot of Fig. 5 below the value for pure PBT). This influence of the crystallinity level is also clear, because if the density of the amorphous PBT was used instead of the used PBT, all the values would appear as above linearity instead of below. The density values of the amorphous part of the blends ( $\rho_a$ , solid squares) also appear below linearity in Figure 7 with the exception of the very rich PC blends. This indicates that an increase in free volume has taken place as a result of blending at low PC contents. This increase is smaller in the case of middle compositions. A decrease in free volume, thus, compaction of the molecular arrangement, has taken place at high PC

contents. Thus, with the exception of the very rich PC blends, the density of the amorphous phases of the blends also separates the density values of the blends from linearity. As a conclusion, with the exception of the very rich PC blends where free volume and crystallinity level changes are opposite, both effects are complementary and concomitant separating density from linearity.

In Figure 8, the moduli of elasticity of the blends are plotted against composition. As can be seen, most of the values give rise to a clear synergism with a maximum at an 80% PC blend composition. Synergisms of this kind are not rare in the case of blends similar to PC/PBT,<sup>22,23</sup> but they have taken place mostly in the case of reacted blends. The importance of this synergism is enhanced by the fact that the plotted modulus of pure PBT has a high reference. This is because its crystalline content, and likely modulus, is higher than that of the PBT in the blends.

The synergism and the modulus maximum at 80% PC can be due to three main possibilities: These are an antiplasticization effect of PBT on PC, the different crystallinity levels of the blends, and a change in the free volume of the blends. With respect to the first possibility, antiplasticization could be due to the depression of the low-temperature transition of



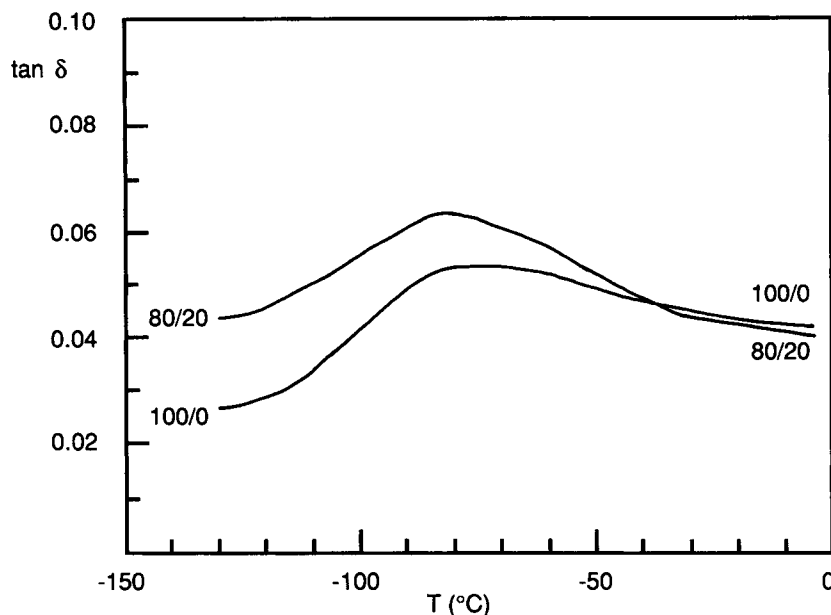


**Figure 9**  $\tan \delta - T$  plot of pure PC and 80/20 PC/PBT blend in the low-temperature range.

PC by PBT. That is why in Figure 9 the low-temperature  $\tan \delta$  values of PC and 80/20 blends are shown. As can be seen, there is no sign of antiplasticization.

With respect to the second possibility, it seems that the percentage of crystallinity is not the reason for the observed modulus behavior (Fig. 8). When the crystalline level remains basically constant between 20 and 60% PC contents (Fig. 5), the curve of the modulus does not show any observable change of shape. This indicates that the crystalline content at these levels scarcely has an effect on modulus behavior. The above comments point to another factor, such as the change in free volume, as the main parameter that determines the modulus behavior. If we look at Figures 7 and 8, we realize that the shapes of both plots are clearly related, although the slight negative deviation from linearity of the middle compositions (solid squares in Fig. 7) does not correspond with the values above linearity of the modulus. This is because the lowest density value of the amorphous blend from linearity, which takes place at a 10% PC, is also the only value of the modulus under linearity. This is because the only values linear or above linearity at a 80–90% PC content give rise to the maximum observed synergism in Figure 8. Thus, the observed results point to the density of the amorphous part of the blend as the main factor that determines the changes in the modulus of elasticity. This is also true even in the case of these partially crystalline blends.

Figure 10 plots the yield stress against composition of the blends. As can be seen, the shape of this

curve is similar to that of the modulus of elasticity. This is because the overall behavior is above linearity although less dynamic than in the case of the moduli of elasticity. Moreover, the decrease in the modulus of elasticity that took place in the 10/90 PC/PBT blends appears again and clearer than before. If we look at the density plot of the amorphous part of the blend in Figure 7, we realize that this small deformation property also seems to be a main consequence of density. This is because, as the density's negative deviation decreases or the positive deviation increases with respect to linearity in Figure 7, the higher both the modulus of elasticity and the yield stress are.

The values of the break stress and ductility are shown in Figures 11 and 12. As can be seen in Figure 11, the break stress shows an unexpected behavior rather similar to those of the modulus and yield stress. Despite the rather large scale used, as in the case of the yield stress, this gives rise to the behavior being more linear than the figure appears to suggest. The almost linearity of both break properties also agrees with the fact that adhesion takes place in these blends just above the glass transition temperature of both resins.<sup>24</sup> Excellent adhesion will probably be promoted by the overall presence of both components of the blend in each amorphous phase, a result of melt blending. This allows the continuity of the material to be maintained not only up to the small elongation characteristics of the modulus of elasticity or yield point, but also up to elongations of rupture typical for any of the components.

In Figure 12, ductility, measured as percent elon-

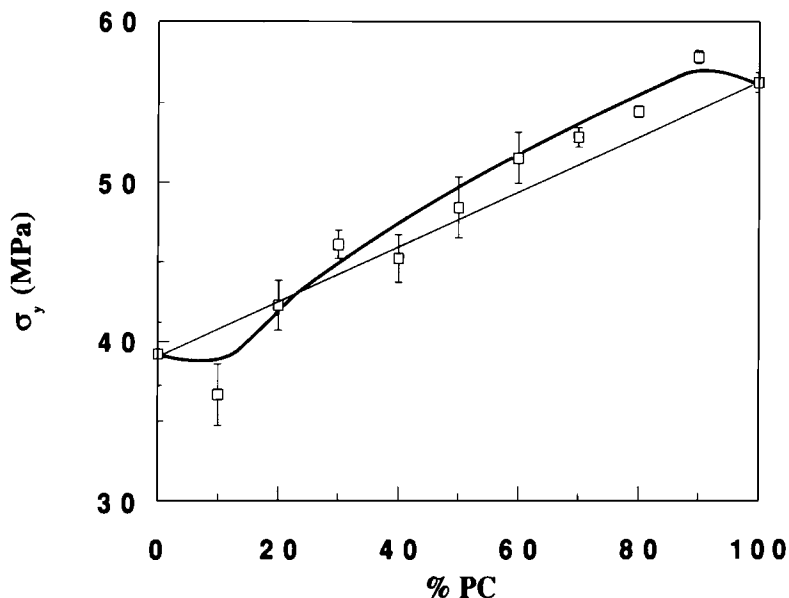


Figure 10 Tensile yield stress vs. composition of the blends.

gation at break, is plotted against blend composition. As can be seen, the ductility values are rather close, but below, linearity. Even a positive deviation from linearity is observed in the 90/10 PC/PBT blend. This is despite the overall positive deviations from linearity observed in the Young's modulus and in the yield stress values. These usually give rise to the opposite behavior in ductility. If we look at Figure 12 in detail, we realize that the behavior is almost the opposite to that observed in the case of the other properties. This is in accordance with the previous statements suggesting the main importance of density of the amorphous blend in properties. Thus, the effect of the change in density or free volume on the

stress-related properties appears to be opposite to that occurring in deformation-related properties like ductility. The biphasic nature of the material does not seem to be a factor for the effect of the free volume to be present. This is due to the effective stress transmission between the phases of the blend that was clearly seen in Figure 6.

## CONCLUSIONS

The PC/PBT blends, although transparent in the melted state and mostly in the solid state, after the followed processing method, are partially miscible

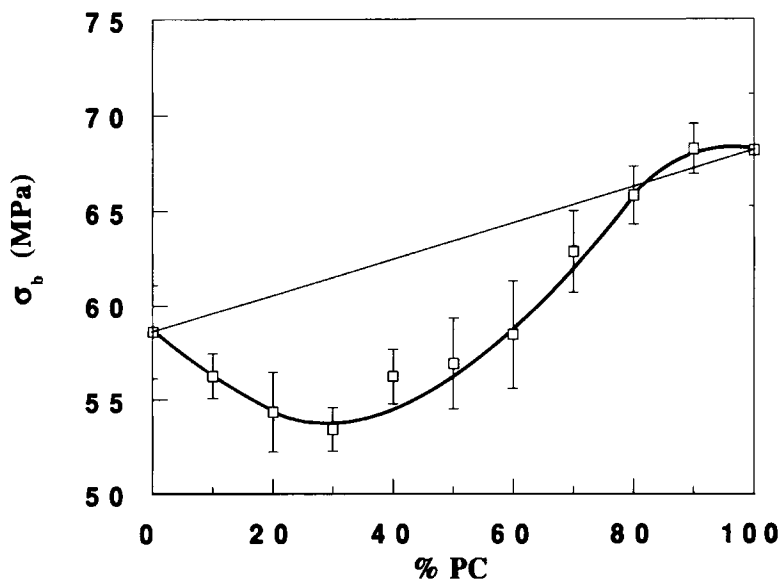


Figure 11 Tensile break stress vs. composition of the blends.

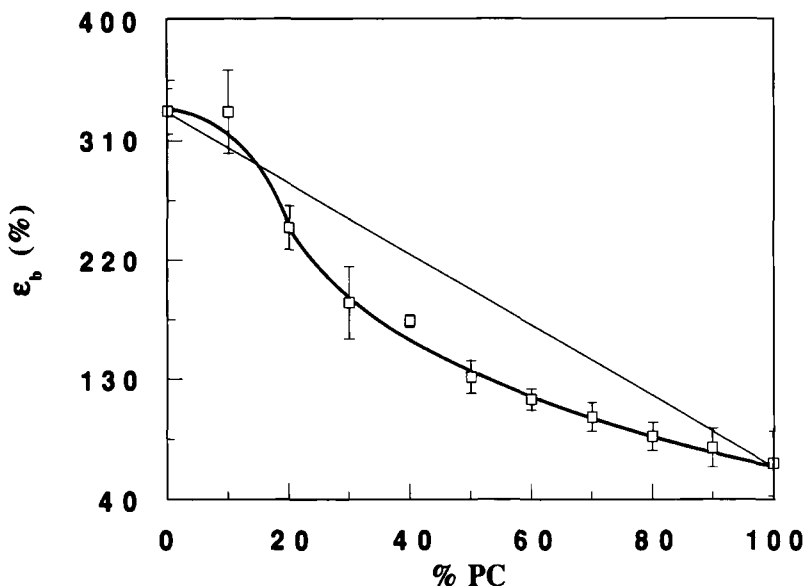


Figure 12

blends. They are composed by a PC-rich phase, an amorphous PBT-rich phase, and a crystalline PBT phase. The crystalline phase increases in volume when heated using PBT crystallized from both amorphous phases.

At the present crystalline levels, crystallinity does not seem to be an important parameter relative to mechanical properties. The free volume of the amorphous part of the blend, however, appears as the main parameter that determines the modulus of elasticity and other mechanical properties even in these partially crystalline blends.

The almost linearity of the break properties and the clear synergisms observed mainly in the modulus of elasticity as well as in the yield stress have been the probable support for the commercialization of some of these blends.

The financial support of the "Gipuzkoako Foru Aldundia" is gratefully acknowledged.

## REFERENCES

1. M. Rappaport, *Plast. Eng.*, **4**, 33 (1985).
2. M. T. Shaw, *Polym. Eng. Sci.*, **22**, 115 (1982).
3. R. S. Porter, J. M. Jonza, M. Kimura, C. R. Desper, and E. R. George, *Polym. Eng. Sci.*, **29**, 55 (1989).
4. R. S. Porter and L.-H. Wang, *Polymer*, **33**, 2019 (1992).
5. A. M. Kotliar, *J. Polym. Sci. Macromol. Rev.*, **16**, 367 (1981).
6. D. C. Wahrmond, D. R. Paul, and J. W. Barlow, *J. Appl. Polym. Sci.*, **22**, 2155 (1978).
7. R. S. Halder, M. Joshi, and A. Misra, *J. Appl. Polym. Sci.*, **39**, 1251 (1990).
8. J. Devaux, P. Godard, and J. P. Mercier, *Polym. Eng. Sci.*, **22**, 229 (1982).
9. S. Y. Hobbs, M. E. J. Dekkers, and V. H. Watkins, *J. Mater. Sci.*, **23**, 1219 (1988).
10. A. W. Birley and X. Y. Chen, *Br. Polym. J.*, **17**, 297 (1985).
11. L. A. Utracki, in *Rheological Measurement*, A. A. Collyer and D. W. Clegg, Eds., Elsevier, London, 1988.
12. L. A. Utracki, *Polym. Eng. Sci.*, **23**, 602 (1983).
13. L. A. Utracki, *Polymer Alloys and Blends*, Hanser, Munich, 1990, Chap. 3.
14. W. N. Kim and C. M. Burns, *Makromol. Chem.*, **190**, 661 (1989).
15. G. J. Pratt and M. J. A. Smith, *Polymer*, **30**, 1113 (1989).
16. H. Bertilsson, B. Franzén, and J. Kubát, *Plast. Rubber Process. Appl.*, **11**, 167 (1989).
17. V. K. Stokes, *Polymer*, **33**, 1237 (1992).
18. S. Y. Hobbs and V. K. Stokes, *Polym. Eng. Sci.*, **31**, 502 (1991).
19. D. Quintens, G. Groeninckx, M. Guest, and L. Aerts, *Polym. Eng. Sci.*, **30**, 1474 (1990).
20. A. F. Yee and M. A. Maxwell, *J. Macromol. Sci. Phys.*, **B17**, 543 (1980).
21. J. Blandrup and E. H. Immergut, Eds., *Polymer Handbook*, Wiley-Interscience, New York, 1989.
22. I. Mondragón and J. Nazábal, *J. Appl. Polym. Sci.*, **32**, 6191 (1986).
23. J. M. Martínez, J. I. Eguiazábal, and J. Nazábal, *J. Appl. Polym. Sci.*, **45**, 1135 (1992).
24. S. Y. Hobbs, U. M. Watkins, and J. T. Bandler, *Polymer*, **31**, 1663 (1990).

Received August 21, 1992

Accepted March 9, 1993